HHS Public Access

Author manuscript

Parkinsonism Relat Disord. Author manuscript; available in PMC 2023 August 01.

Published in final edited form as:

Parkinsonism Relat Disord. 2022 August ; 101: 31–38. doi:10.1016/j.parkreldis.2022.06.015.

Reduced gene dosage is a common mechanism of neuropathologies caused by ATP6AP2 splicing mutations

William C. Edelman, Ph.D.[1], **Kostantin Kiianitsa, Ph.D.**[2], **Tuhin Virmani, M.D., Ph.D.**[3], **Refugio A. Martinez, B.S.**[4,5], **Jessica E. Young, Ph.D.**[4,5], **C. Dirk Keene, M.D., Ph.D.**[4], **Thomas D. Bird, M.D.**[6,7], **Wendy H. Raskind, M.D., Ph.D.**[1,8,9], **Olena Korvatska, Ph.D.**[8,9,*]

[1] -Division of Medical Genetics, Department of Medicine, University of Washington, Seattle, Washington, USA

[2] -Department of Immunology, University of Washington, Seattle, Washington, USA

[3] -Department of Neurology, University of Arkansas for Medical Sciences, Little Rock, Arkansas, USA

[4] -Department of Laboratory Medicine and Pathology, University of Washington, Seattle, Washington, USA

[5] -Institute for Stem Cell and Regenerative Medicine, University of Washington, Seattle, Washington, USA

[6] -Department of Neurology, University of Washington, Seattle, Washington, USA

[7] -Geriatric Research, Education and Clinical Center (GRECC), VA Puget Sound Medical Center, Seattle, Washington, USA

[8] -Department of Psychiatry and Behavioral Sciences, University of Washington, Seattle, USA

[9] –Mental Illness Research, Education and Clinical Center (MIRECC), VA Puget Sound Medical Center, Seattle, Washington, USA

Abstract

Background.—Mutations that alter splicing of X-linked *ATP6AP2* cause a spectrum of neurodevelopmental and neurodegenerative pathologies including parkinsonism in affected males. All previously reported splicing mutations increase the level of a minor isoform with skipped exon 4 (Δe4) that encodes a functionally deficient protein.

Objectives.—We investigated the pathogenic mechanism of a novel c.168+6T>A variant reported in a family with X-linked intellectual disability, epilepsy, and parkinsonism. We also

*Corresponding author: Olena Korvatska, ok5@uw.edu.

Authors contribution:
O.K., W.H.R., T.D.B., J.E.Y. – conception and design of the study,
T.V., T.D.B., C.D.K., - sample acquisition and ascertainment,
W.C.E., R.A.M., O.K. – acquisition of data,
W.C.E., K.K., O.K. -analysis and interpretation of data,
W.C.E., K.K., O.K., W.H.R. – drafting the manuscript,
K.K., T.D.B., W.H.R., O.K. – revising the manuscript

Declarations of competing interest: none

analyzed *ATP6AP2* splicing defects in brains of carriers of a c.345C>T variant associated with X-linked spasticity and parkinsonism.

Methods.—We generated induced pluripotent stem cells from patients with c.168+6T>A, reprogrammed them to neural progenitor cells and analyzed them by RNA-Seq and qRT-PCR. We also quantified *ATP6AP2* isoforms in the brains of c.345C>T carriers by Nanostring nCounter.

Results.—The c.168+6T>A increased skipping of *ATP6AP2* exon 2 and usage of cryptic intronic donor splice sites. This results in out-of-frame splicing products and a reciprocal 50% reduction in functional full-length ATP6AP2 transcripts. Neural progenitors of patients with c.168+6T>A exhibited downregulated neural development gene networks. Analysis of blood transcriptomes of c.168+6T>A carriers identified potential biomarkers of ATP6AP2 deficiency in non-neural tissues. The c.345C>T variant increased exon 4 skipping with concomitant decrease of full length *ATP6AP2* in brains of carriers.

Conclusion.—A common pathogenic consequence of splicing mutations affecting inclusion of different *ATP6AP2* exons is reduction of the functional full-length transcript. The exacerbated *ATP6AP2* splicing defect in brains of c.345C>T carriers is consistent with their CNS-restricted clinical presentations.

Keywords

Alternative splicing; vacuolar H^+ ATPase

1. INTRODUCTION.

ATP6AP2 is an essential X-linked gene encoding a transmembrane protein that enables assembly of vacuolar H^+ ATPase (V-ATPase) [1], a multi-protein complex with lysosomal, autophagosomal and intracellular pH maintenance functions [2]. Mutations that affect *ATP6AP2* splicing cause a spectrum of neurological disorders manifesting as cognitive and/or movement impairments (spasticity and parkinsonism) in affected males. Synonymous variants in *ATP6AP2* exon 4, c.321C>T and c.345C>T, reported in families with X-linked mental retardation Hedera type [3] (MRXSH) and X-linked parkinsonism with spasticity [4] (XPDS), respectively, dramatically increased exon 4 skipping resulting in overproduction of a non-functional isoform, Δe4, that lacks the 32 amino acids encoded by exon 4 [5]. Recently, a *de novo* intronic indel mutation, c.301-11_301-10delTT, affecting exon 4 skipping was described in a child with a fulminant form of neurodegeneration [6]. A distinct intronic variant, c.168+6T>A, predicted to affect *ATP6AP2* exon 2 splicing was found in a family with parkinsonism, epilepsy and intellectual disability [7]. Herein, we report characterization of the molecular effect of c.168+6T>A on *ATP6AP2* splicing and effect on expressed gene networks in peripheral blood and neural progenitor cells established from members of this family. We found that c.168+6T>A increased exon 2 skipping and usage of cryptic intronic splice sites; the resulting isoforms decreased the functional *ATP6AP2* transcript by splicing competition. Integrative gene network analysis revealed neural development pathways downregulated by the decreased *ATP6AP2* level in neural progenitor cells. We also found that the level of functional full length *ATP6AP2* was

profoundly reduced in brains of c.345C>T carriers because of competition with the Δe4 isoform.

2. METHODS.

2.1. Subjects.

The study was carried out in accordance with The Code of Ethics of the World Medical Association (Declaration of Helsinki) for experiments involving humans http://www.wma.net/en/30publications/10policies/b3/index.html; and Uniform Requirements for manuscripts submitted to Biomedical journals (http://www.icmje.org). Under protocols approved by the Institutional Review Board of the University of Washington, all subjects had previously given informed consent to share and study live cells and autopsy material. All methods for processing and analyzing this biological material were in accordance with relevant guidelines and regulations.

We obtained peripheral blood from two patients and their mother with *ATP6AP2* c.168+6T>A [7] and from normal control subjects (N=6) and formalin fixed paraffin embedded (FFPE) autopsy tissues from an XPDS patient (II-2) and a female-carrier (II-8) with the c.345C>T variant [8] (Fig. S1). AD cases and aged non-demented controls were obtained from the UW Neuropathology Core Brain Bank (Table S1).

2.2. Generation of iPSCs and their reprogramming to neural lineage.

Peripheral blood mononuclear cells (PBMCs) from two affected brothers [7] and two non-affected unrelated males were converted into induced pluripotent stem cells (iPSC) using a non-integrating CytoTune Sendai viral re-programming kit (A16517, Thermo Fisher) according to the manufacturer's instructions. Briefly, 5 x 10^5 PBMCs were transduced with the virus at multiplicity of infection 5. After 48 hr, media was replaced, and cells were passaged till iPSC colonies appeared (days 12-25). Colonies were manually picked and plated onto gamma ray-irradiated in-house prepared mouse embryonic fibroblasts in KO-SR medium composed of DMEM/F12 culture medium (11320033, Thermo Fisher) supplemented with 20% KnockOut Serum Replacement, 0.1 mmol/l non-essential amino acids, 1 mmol/l l-glutamine, 0.1 mmol/l 2-mercaptoethanol, penicillin/streptomycin (Thermo Fisher), and 12.5 ng/ml recombinant human basic FGF (130-093-839, Miltenyi Biotec). Following expansion, iPSC colonies were selected by morphology and expression of pluripotency markers OCT4, Tra1-60 and SSEA4 (Fig.S1A), and passaged 3 times on Matrigel-coated plates (# 356231, Corning, NY). iPSCs were differentiated to NPCs using a previously described modification of dual-SMAD inhibition protocol [9]. Briefly, iPSCs were plated on Matrigel-coated 6-well plates at a density of 3.5 million cells per well. Cells were grown in Basal Neural Maintenance Media (1:1 DMEM/F12, #11039047 Life Technologies) supplemented with glutamine media/neurobasal media (#21103049, GIBCO), 0.5% N2 supplement (#17502–048, Thermo Fisher), 1% B27 supplement (# 17504–044, Thermo Fisher), 0.5% GlutaMax (# 35050061, Thermo Fisher), 0.5% insulin-transferrin-selenium (#41400045, Thermo Fisher), 0.5% NEAA (# 11140050, Thermo Fisher), 0.2% β-mercaptoethanol (#21985023, Life Technologies), 10 μM SB-431542 and 0.5 μM LDN-193189 (#1062443, Biogems). The media was exchanged daily for seven days.

On day eight, cells were incubated with Versene (#15640066, GIBCO), gently dissociated using cell scrapers, and split 1:3. On day nine, media was switched to Basal Neural Maintenance Media containing 20 ng/mL FGF (R&D Systems, Minneapolis, MN). The media was exchanged daily. On day sixteen, cells were passaged 1:3 and grown with daily media change until formation of neural rosettes, approximately day twenty-three. At this time, cells were FACS sorted with four markers (CD184, CD24, CD44 and CD271 (#557145, #561646, #555479, #557196, BD PharMingen) to obtain pure populations of NPCs ($CD184^+/CD24^+/CD44^-/CD271^-$) [10]. Following sorting, NPCs were expanded, and their identity was confirmed by staining with NPC markers nestin and TBR2 (Fig. S1B). Genomic integrity was assessed by karyotyping (Fig. S1C). The presence of the intronic c.168+6T>A variant in *ATP6AP2* was confirmed by Sanger sequencing.

2.3. Lymphoblastoid cell lines (LCLs).

Epstein-Barr virus transformed LCL were established from PBMC of patients and male controls who carry a reference *ATP6AP2* allele, as described previously [11], and cultured in RPMI medium supplemented with 10% fetal bovine serum. Cells were treated with cycloheximide (Sigma, 100 μg/ml) for the indicated time.

2.4. RNA isolation and qRT-PCR analysis.

Total RNA from blood (PBMC), LCL and NPC was isolated using the RNAeasy kit (#74106, Qiagen) and quantitated by Qubit Fluorometer (Molecular Probes). RNA integrity number (RIN) was measured by TapeStation (Agilent Technologies). cDNA was synthesized with SensiFast (BIO-65053, Bioline). The following RT-PCR primers were used: Forward: 5'-CATGGCTGTGTTTGTCGTG-3' and reverse: 5'- TCTCCAAAGGGTACGAAATGA −3' (located within *ATP6AP2* exon 1 and exon 3, respectively). TaqMan® Fast Advanced Master Mix and the following TaqMan Gene Expression Assays were used for qRT-PCR: Hs00366626_m1, Hs00997140_g1 and Hs00997145_m1 for exon 1-2; e3-4 and e8-9 junctions of *ATP6AP2*. For reference genes (*TBP* and *GUSB*), Hs00427620_m1 and Hs00939627_m1 were used, respectively. Assays were performed on a StepOnePlus real time PCR machine and analyzed with StepOne software (Applied Biosystems) using the 2(-Delta Delta C(T)) method [12].

2.5. Gene expression analysis by NanoString nCounter.

Total RNA was isolated from four 10 μm thick FFPE sections using the Recover All RNA isolation kit (Ambion). RNA (1 μg) was hybridized with the PanCancer Immune panel (730 cancer/immunity related genes and 40 housekeeping genes) supplemented with a probe to *ATP6AP2* exon 3/5 junction (detects Δe4 only) and a probe to the invariant exon 8/9 junction (detects total *ATP6AP2*). Data were normalized using the nSolver 3.0 Analysis Software (NanoString Technologies). Expression of full length *ATP6AP2* was calculated by subtracting the level of the Δe4 transcript (measured by e3-5 probe) from that of total *ATP6AP2* transcript (measured by e8 probe to invariant exon present in both isoforms).

2.6. RNA-seq.

RNA samples with a RIN > 8 were used for sequencing library construction. Generation of strand-specific mRNA libraries and sequencing were performed using BGI services. cDNA libraries were sequenced on a DNBSEQ platform using a paired-end strategy (read length 150 bp) with sequencing depth of 40 million clean reads per sample. Raw reads were aligned to the human genome, version GCF_000001405.38_GRCh38.p12, using HISAT and Bowtie2. All samples had Pearson's correlation coefficients above 0.85 confirming absence of outliers due to RNA sample or sequencing library quality. Differential gene expression analysis was performed using the DESeq2. Differentially expressed genes (DEGs) were selected based on q-value threshold of 0.05.

2.7. Bioinformatic and statistical analyses.

To identify biologically relevant pathways in sets of differentially expressed genes, we used Metascape [13] and Doctor Tom software (BGI). The following ontology sources were queried: GO Biological Processes, Reactome Gene Sets, KEGG Pathway, Canonical Pathways, CORUM, TRRUST, DisGeNET, PaGenBase, Transcription Factor Targets, WikiPathways and PANTHER Pathway. Protein-protein interactions (PPI) enrichment analysis was carried out using STRING, BioGrid, OmniPath and InWeb_IM databases [13]. Other statistical tests were performed using GraphPad Prism software.

3. RESULTS

3.1. c.168+6T>A mutation alters ATP6AP2 splicing leading to reduced dosage of functional transcript

The intronic c.168+6T>A variant in *ATP6AP2* in patients with X-linked intellectual disability, epilepsy, and parkinsonism [7] is predicted by SpliceAI [14] and MMSp [15] to weaken the exon 2 donor splice site and has a pathogenicity score (CADD score, [16]) of 12.9. Consequently, exon 2 may be either completely excluded (skipping) or modified via use of a cryptic donor splice site. To investigate effects of c.168+6T>A on *ATP6AP2* splicing in patient cells, we isolated RNA from PBMCs of two affected males. Analysis of RT-PCR products amplified with primers located on *ATP6AP2* exons 1 and 3 identified an additional band of lower molecular weight in 168+6T>A carriers (Fig 1A). Sequencing of the gel-purified fragment showed an exact exon 1/3 junction thus confirming the exon 2 skipping mechanism (Fig.1B). To determine if overproduction of the Δe2 isoform depletes the functional full length (FL) ATP6AP2 transcript by splicing competition we used junction-specific qRT-PCR assays that can distinguish these isoforms (Fig.1C). A probe to the e1/2 junction specific for the FL transcript detected its 50% decrease in PBMC of patients. Interestingly, e3/4 and e8/9 probes that detect both FL and Δe2 showed a decrease of total ATP6AP2 transcript in patients, suggesting that the Δe2 transcript has decreased stability.

3.2. Δe2 ATP6AP2 is differentially regulated by nonsense-mediated RNA decay.

The exon 1/3 splice junction introduces a frame shift resulting in a premature stop codon at amino acid 23 (Fig. 1B) that may be subject to nonsense-mediated RNA decay (NMD).

Alternatively, the Δe2 transcript may escape NMD by using in-frame ATG codons in the exon 3 sequence. To determine whether NMD affects the Δe2 level we used LCLs established from patients who carry the *c.168+6T>A mutation* and controls who do not. Cells were treated with cycloheximide (CHI), a potent inhibitor of eukaryotic translation and NMD. Analysis of RT-PCR products amplified with primers to exons 1 and 3 demonstrated a robust Δe2 band in patients and a minute amount of this product in control LCLs (Fig. 2). NMD inhibition by CHI in patient cells revealed accumulation of a band migrating above the FL product. Sequencing revealed a heterogeneous mix of species with a major product containing spliced exons 1, 2, 3 and a retained part of intron 2 sequence (Fig. S2). This indicates that the *c.168+6T>A* mutation generates multiple aberrant splicing products which outcompete the functional FL transcript. However, CHI treatment had little effect on the Δe2 transcript indicating that this isoform likely escapes NMD in LCLs. qRT-PCR analysis with three junction specific probes (Fig. 1D) found a decrease of FL isoform (e1/2 probe), while the total ATP6AP2 transcript (e3/4 and e8/9 probes) was unchanged, consistent with escape of Δe2 from NMD in LCL.

3.3. ATP6AP2 reduced by aberrant exon 2 splicing perturbs neural development gene networks in iPSC-derived NPCs of patients with c.168+6T>A

To study the effect of *ATP6AP2* c.168+6T>A splicing mutation in a neuronal context, we generated iPSCs from PBMCs of patients carrying 168+6T>A and normal control males and reprogrammed them to NPCs. iPSCs were differentiated into neural lineage through a modified dual SMAD inhibition protocol [9], [17] until rosette-like structures emerged. To enrich for the NPC population, we used FACS sorting with four lineage-specific markers (CD184+/CD271-/CD44-/CD24+) [10]. NPC identity of post-sorted cells was additionally confirmed by staining with NPC markers nestin and TBR2 (Fig. S1). We identified a robust band of Δe2 RT-PCR product and a 2-fold decrease of FL *ATP6AP2* transcript in NPC of 168+6T>A carriers (Fig. 3A-B). Similar to LCL, we did not observe a significant decrease of total ATP6AP2 transcript in carriers suggesting that Δe2 escapes NMD in NPC as well. To characterize gene networks affected by reduced ATP6AP2 dosage, we performed mRNA-Seq of NPCs of patients (7 lines established from 2 patients with c.168+6T>A allele) and controls (6 lines from 2 normal males with the reference allele) (Table S1 and Fig. S3). Of the 1,038 differentially expressed genes (DEGs), 505 were upregulated and 533, including *ATP6AP2* itself, were downregulated. Pathway and process enrichment analysis identified top pathways perturbed by the reduced *ATP6AP2* dosage (Fig. 3, Tables S2 and S3 [13]): The top upregulated pathways were related to extracellular matrix (ECM) function, such as ECM organization, cell adhesion, junctions and ECM protein digestion, whereas the top downregulated pathways were related to neural system (neuronal/glial fate, pattern specification, synapse assembly and signaling). Notably, markers of neuronal and glial development (*ISL1, NKX2-1, OLIG2, OLIG1, DBX1*), synaptic transmission (*GABRA3, GABRB1, GRIK3, HTR2C, PDYN, GABBR2, SLC4A10*) and pattern specification (*FGF8, ISL1, OTX1, NKX21, ZIC1, EOMES, DBX1, HELT*) were among the top 50 downregulated genes (5% of down DEGs). Analysis of protein-protein interaction (PPI) networks pinpointed several modules related to pathways previously reported as affected by ATP6AP2 deficit (Fig. S4). This included WNT signaling [18], [19] vesicular transportation ER to Golgi [5], [20] and metabolic glucose switch [21].

Other perturbed networks of proteins included upregulation of post-translational protein modification and organization of tight junctions.

3.4. Blood transcriptome reveals neural disease-associated genes affected by ATP6AP2 deficiency

ATP6AP2 is an accessory component of the V-ATPase complex and is an essential, ubiquitously expressed housekeeping gene, yet the pathogenicity of aberrant *ATP6AP2* splicing is confined to the CNS. Because the functional *ATP6AP2* transcript is also substantially reduced in blood of c.168+6T>A carriers we asked whether expression signatures in non-neural cells may be informative of the ATP6AP2 deficiency mechanism. To this end, we performed mRNA-Seq analysis of blood RNA of three c.168+6T>A carriers, two affected male patients and their unaffected mother, comparing them with sex-matched unrelated normal individuals (2 males and 2 females). 38 DEGs were identified, including the downregulated *ATP6AP2* (Fig S5). Notably, *ATP6AP2* was the only DEG located within the critical XPDS linkage region demonstrating that transcriptomes of non-neural cells may be informative in pinpointing CNS disease genes affected by mutations that change their expression or splicing. Only three DEGs of the blood transcriptome, including the ATP6AP2, overlapped with the NPC; also, top pathways dysregulated in NPC did not overlap with the blood ones (Fig. S6). To identify a connection of blood DEGs to neurological conditions we performed a Metascape search against the DisGeNET database of gene-disease associations [22]. Twelve DEGs were associated with neurological diseases or syndromes (Table 1). Notably, the *HDC* gene encoding histidine decarboxylase is downregulated in both blood and NPC transcriptomes. *HDC* has been implicated in Gilles de la Tourette syndrome (OMIM # 137580), a disorder with neurobehavioral and movement manifestations.

3.5. Competition with the Δe4 splice isoform leads to a severe reduction of functional full length ATP6AP2 transcript in XPDS brain

Molecular analysis of previously characterized *ATP6AP2* splicing mutations revealed overproduction of a potentially deleterious Δe4 isoform. In non-neural tissues of XPDS patients, such as blood, we found that Δe4 competed with the FL isoform effectively reducing the level of the latter [4]. To assess the effect of ATP6AP2 splice isoform competition in the CNS, we measured Δe4 and FL isoforms in brains of two c.345C>T carriers from the XPDS family: a previously characterized male patient and a female relative whose autopsy recently became available (II-2 and II-8 in Fig. S4 [8]). Neurologic examination of the female carrier at age 78 had not revealed XPDS features, such as tremor, rigidity, abnormal reflexes, or parkinsonism. By age 84, she developed cognitive impairment and eventually entered a nursing home where she died at age 90 with advanced dementia. Neuropathological examination of her brain confirmed Alzheimer's disease. We isolated RNA from hippocampal FFPE sections of these two subjects and measured *ATP6AP2* isoforms by Nanostring nCounter using a probe to the exon 3/5 junction, which detects Δe4, and a probe to the invariant exon 8, which detects both full length and Δe4 isoforms. For comparison, we used age-matched normal controls (N=17) and patients with sporadic AD (N=15) (Table S1). Quantification of total *ATP6AP2* revealed its consistently high expression in brain but no difference between groups (Fig. 4A). Δe4 level did not differ

between normal and AD groups, averaging 5% of total ATP6AP2, consistent with previous measurement by qRT-PCR of flash-frozen brain samples [4]. In c.345C>T carriers, Δe4 increased substantially and it became the major ATP6AP2 isoform (Fig. 4B). Consequently, full length *ATP6AP2* was dramatically reduced in c.345C>T carriers, down to 5% in the XPDS patient and 33% in the female carrier but was not significantly changed in the AD group (Fig. 4C).

4. DISCUSSION.

Prior studies of molecular phenotypes of CNS pathology-causing splicing mutations in *ATP6AP2* pointed to the overproduction of the isoform with skipped exon 4, Δe4, as a key event that may drive neuropathology [3, 4, 6]. Δe4 encodes a protein with 32 amino acids deleted from the ectodomain that is unable to complement essential ATP6AP2 functions [5]. Due to the competitive nature of splicing, Δe4 overproduction is expected to deplete the functional ATP6AP2 isoform, but this had not been quantified for all disease-causing mutations, particularly in CNS cells and tissues. Independently, Δe4 overexpression *per se* may negatively affect neural differentiation via formation of inactive ATP6AP2 dimer, as demonstrated in the rat PC-12 model of neurogenesis [23]. Herein, we addressed (1) the contribution of splicing isoform competition as the mechanism for depletion of functional ATP6AP2 transcripts in the brain of carriers of an XPDS mutation, c.345C>T, known to increase exon 4 skipping and (2) investigated a yet unclear mechanism of splicing changes caused by the c.168+6T>A variant found in a family with X-linked intellectual disability, epilepsy, and parkinsonism. We established that c.168+6T>A, predicted to weaken the donor splice site for exon 2, resulted in several defects of exon 2 splicing, such as exon skipping and usage of a cryptic donor site in intron 2. The overproduction of these aberrant isoforms led to depletion of a functional full-length transcript in both non-neural cells and iPSC-derived NPCs of patients. Several naturally occurring minor ATP6AP2 transcript isoforms with skipped exon 2 are annotated in human RNA splicing databases (Ensembl, GTEx). The most common one, ENST00000637327.1 (ATP6AP2-224) is a predicted protein-coding transcript with an alternative ATG codon in exon 3, encoding a polypeptide with 76 missing N-terminal residues. Because the exon 1/3 splice junction introduces a frame shift with a stop codon, Δe2 may be subject to differential regulation at the post-transcriptional level, either by undergoing NMD or escaping it. Regardless the Δe2 post-transcriptional fate, its overproduction ultimately leads to decreased dosage of a functional ATP6AP2 transcript due to splicing competition.

At a systems level, a 50% decrease of full-length *ATP6AP2* in NPCs of patients caused downregulation of networks related to neuron fate commitment, axon guidance and CNS neuron differentiation highlighting the sensitivity of neural cells to even moderate change in ATP6AP2 dosage. Interestingly, studies of iPSC-derived neurons and astrocytes from a patient with fulminant neurodegeneration, in which c.301-11_301-10delTT severely skewed the Δe4/full-length isoform ratio [6] also found defective neural differentiation. The defects were rescued by full length ATP6AP2 overexpression suggesting that the isoform competition depleted the full-length transcript. To measure the magnitude of effect of exon 4 skipping on full-length *ATP6AP2* level in CNS tissues, we quantified ATP6AP2 isoforms in brains of carriers of the exon 4 skipping mutation that causes XPDS. While the total level of

ATP6AP2 transcripts was not changed in carriers, Δe4 overexpression dramatically reduced the full-length transcript confirming the isoform competition mechanism of pathology.

We acknowledge limitations imposed by the rarity of the genetic variants and diseases under study that engender the low number of affected brain tissues and live cells from patients, as well as use of non-isogenic controls. Given the inherent variability of the iPSC differentiation process and limited number of neural progenitor lines, only the most up/down-regulated pathways could be identified. Future studies in brain organoid models or in brain tissues of patients would be valuable to confirm and extend our findings.

In summary, we found that the molecular phenotype of *ATP6AP2* splicing mutations that cause a spectrum of congenital neurodevelopmental and neurodegenerative conditions ultimately converged onto reduction of the full length ATP6AP2 isoform, to which the CNS has a particular sensitivity. This raises an important question about the potential contribution of other known genetic and epigenetic regulators of *ATP6AP2* gene dosage in brain health and disease [24].

Supplementary Material

Refer to Web version on PubMed Central for supplementary material.

Acknowledgments:

We are grateful to the members of the families for their generous donations of cells and tissues for the research. We are thankful to Chris Cavanaugh of the Ellison Stem Cell core for his help with PBMC reprogramming to iPSCs. The work was supported by National Institute of Health [grants T32 AG052354 to W.C.E.; 2R01 NS069719 to W.H.R.], the United States (U.S.) Department of Veterans Affairs Clinical Sciences R&D (CSRD) Service [Merit Review Award Number 101 CX001702 to W.H.R. and O.K.] and the Takayama family gift to O.K.

Data Availability Statement.

mRNA-Seq data generated in this work will be deposited in the Gene Expression Omnibus (GEO) database at the NCBI, after the formal manuscript acceptance for publication and according to data sharing policies of the University of Washington.

References.

1. Abbas YM, Wu D, Bueler SA, Robinson CV, Rubinstein JL (2020) Structure of V-ATPase from the mammalian brain. Science 367, 1240–1246. [PubMed: 32165585]
2. Collins MP and Forgac M (2020) Regulation and function of V-ATPases in physiology and disease. Biochim Biophys Acta Biomembr 1862, 183341. [PubMed: 32422136]
3. Ramser J, Abidi FE, Burckle CA, Lenski C, Toriello H, Wen G, Lubs HA, Engert S, Stevenson RE, Meindl A, Schwartz CE, Nguyen G (2005) A unique exonic splice enhancer mutation in a family with X-linked mental retardation and epilepsy points to a novel role of the renin receptor. Human molecular genetics 14, 1019–27. [PubMed: 15746149]
4. Korvatska O, Strand NS, Berndt JD, Strovas T, Chen DH, Leverenz JB, Kiianitsa K, Mata IF, Karakoc E, Greenup JL, Bonkowski E, Chuang J, Moon RT, Eichler EE, Nickerson DA, Zabetian CP, Kraemer BC, Bird TD, Raskind WH (2013) Altered splicing of ATP6AP2 causes X-linked parkinsonism with spasticity (XPDS). Human molecular genetics 22, 3259–68. [PubMed: 23595882]

5. Kinouchi K, Ichihara A, Sano M, Sun-Wada GH, Wada Y, Ochi H, Fukuda T, Bokuda K, Kurosawa H, Yoshida N, Takeda S, Fukuda K, Itoh H (2013) The role of individual domains and the significance of shedding of ATP6AP2/(pro)renin receptor in vacuolar H(+)-ATPase biogenesis. PloS one 8, e78603. [PubMed: 24223829]
6. Hirose T, Cabrera-Socorro A, Chitayat D, Lemonnier T, Feraud O, Cifuentes-Diaz C, Gervasi N, Mombereau C, Ghosh T, Stoica L, Bacha JDA, Yamada H, Lauterbach MA, Guillon M, Kaneko K, Norris JW, Siriwardena K, Blaser S, Teillon J, Mendoza-Londono R, Russeau M, Hadoux J, Ito S, Corvol P, Matheus MG, Holden KR, Takei K, Emiliani V, Bennaceur-Griscelli A, Schwartz CE, Nguyen G, Groszer M (2019) ATP6AP2 variant impairs CNS development and neuronal survival to cause fulminant neurodegeneration. The Journal of clinical investigation 129, 2145–2162. [PubMed: 30985297]
7. Gupta HV, Vengoechea J, Sahaya K, Virmani T (2015) A splice site mutation in ATP6AP2 causes X-linked intellectual disability, epilepsy, and parkinsonism. Parkinsonism & related disorders.
8. Poorkaj P, Raskind WH, Leverenz JB, Matsushita M, Zabetian CP, Samii A, Kim S, Gazi N, Nutt JG, Wolff J, Yearout D, Greenup JL, Steinbart EJ, Bird TD (2010) A novel X-linked four-repeat tauopathy with Parkinsonism and spasticity. Movement disorders : official journal of the Movement Disorder Society 25, 1409–17. [PubMed: 20629132]
9. Rose SE, Frankowski H, Knupp A, Berry BJ, Martinez R, Dinh SQ, Bruner LT, Willis SL, Crane PK, Larson EB, Grabowski T, Darvas M, Keene CD, Young JE (2018) Leptomeninges-Derived Induced Pluripotent Stem Cells and Directly Converted Neurons From Autopsy Cases With Varying Neuropathologic Backgrounds. Journal of neuropathology and experimental neurology 77, 353–360. [PubMed: 29474672]
10. Yuan SH, Martin J, Elia J, Flippin J, Paramban RI, Hefferan MP, Vidal JG, Mu Y, Killian RL, Israel MA, Emre N, Marsala S, Marsala M, Gage FH, Goldstein LS, Carson CT (2011) Cell-surface marker signatures for the isolation of neural stem cells, glia and neurons derived from human pluripotent stem cells. PloS one 6, e17540. [PubMed: 21407814]
11. Raskind WH, Tirumali N, Jacobson R, Singer J, Fialkow PJ (1984) Evidence for a multistep pathogenesis of a myelodysplastic syndrome. Blood 63, 1318–23. [PubMed: 6326894]
12. Livak KJ and Schmittgen TD (2001) Analysis of relative gene expression data using real-time quantitative PCR and the 2(-Delta Delta C(T)) Method. Methods 25, 402–8. [PubMed: 11846609]
13. Zhou Y, Zhou B, Pache L, Chang M, Khodabakhshi AH, Tanaseichuk O, Benner C, Chanda SK (2019) Metascape provides a biologist-oriented resource for the analysis of systems-level datasets. Nature communications 10, 1523.
14. Jaganathan K, Kyriazopoulou Panagiotopoulou S, McRae JF, Darbandi SF, Knowles D, Li YI, Kosmicki JA, Arbelaez J, Cui W, Schwartz GB, Chow ED, Kanterakis E, Gao H, Kia A, Batzoglou S, Sanders SJ, Farh KK (2019) Predicting Splicing from Primary Sequence with Deep Learning. Cell 176, 535–548 e24. [PubMed: 30661751]
15. Cheng J, Nguyen TYD, Cygan KJ, Celik MH, Fairbrother WG, Avsec Z, Gagneur J (2019) MMSplice: modular modeling improves the predictions of genetic variant effects on splicing. Genome Biol 20, 48. [PubMed: 30823901]
16. Rentzsch P, Witten D, Cooper GM, Shendure J, Kircher M (2019) CADD: predicting the deleteriousness of variants throughout the human genome. Nucleic acids research 47, D886–D894. [PubMed: 30371827]
17. Chambers SM, Fasano CA, Papapetrou EP, Tomishima M, Sadelain M, Studer L (2009) Highly efficient neural conversion of human ES and iPS cells by dual inhibition of SMAD signaling. Nature biotechnology 27, 275–80.
18. Cruciat CM, Ohkawara B, Acebron SP, Karaulanov E, Reinhard C, Ingelfinger D, Boutros M, Niehrs C (2010) Requirement of prorenin receptor and vacuolar H+-ATPase-mediated acidification for Wnt signaling. Science 327, 459–63. [PubMed: 20093472]
19. Hermle T, Saltukoglu D, Grunewald J, Walz G, Simons M (2010) Regulation of Frizzled-dependent planar polarity signaling by a V-ATPase subunit. Curr Biol 20, 1269–76. [PubMed: 20579879]
20. Guida MC, Hermle T, Graham LA, Hauser V, Ryan M, Stevens TH, Simons M (2018) ATP6AP2 functions as a V-ATPase assembly factor in the endoplasmic reticulum. Mol Biol Cell 29, 2156–2164. [PubMed: 29995586]

21. Kanda A, Noda K, Ishida S (2015) ATP6AP2/(pro)renin receptor contributes to glucose metabolism via stabilizing the pyruvate dehydrogenase E1 beta subunit. The Journal of biological chemistry 290, 9690–700. [PubMed: 25720494]

22. Pinero J, Bravo A, Queralt-Rosinach N, Gutierrez-Sacristan A, Deu-Pons J, Centeno E, Garcia-Garcia J, Sanz F, Furlong LI (2017) DisGeNET: a comprehensive platform integrating information on human disease-associated genes and variants. Nucleic acids research 45, D833–D839. [PubMed: 27924018]

23. Contrepas A, Walker J, Koulakoff A, Franek KJ, Qadri F, Giaume C, Corvol P, Schwartz CE, Nguyen G (2009) A role of the (pro)renin receptor in neuronal cell differentiation. American journal of physiology. Regulatory, integrative and comparative physiology 297, R250–7.

24. Colacurcio DJ and Nixon RA (2016) Disorders of lysosomal acidification-the emerging role of v-ATPase in aging and neurodegenerative disease. Ageing Res Rev.

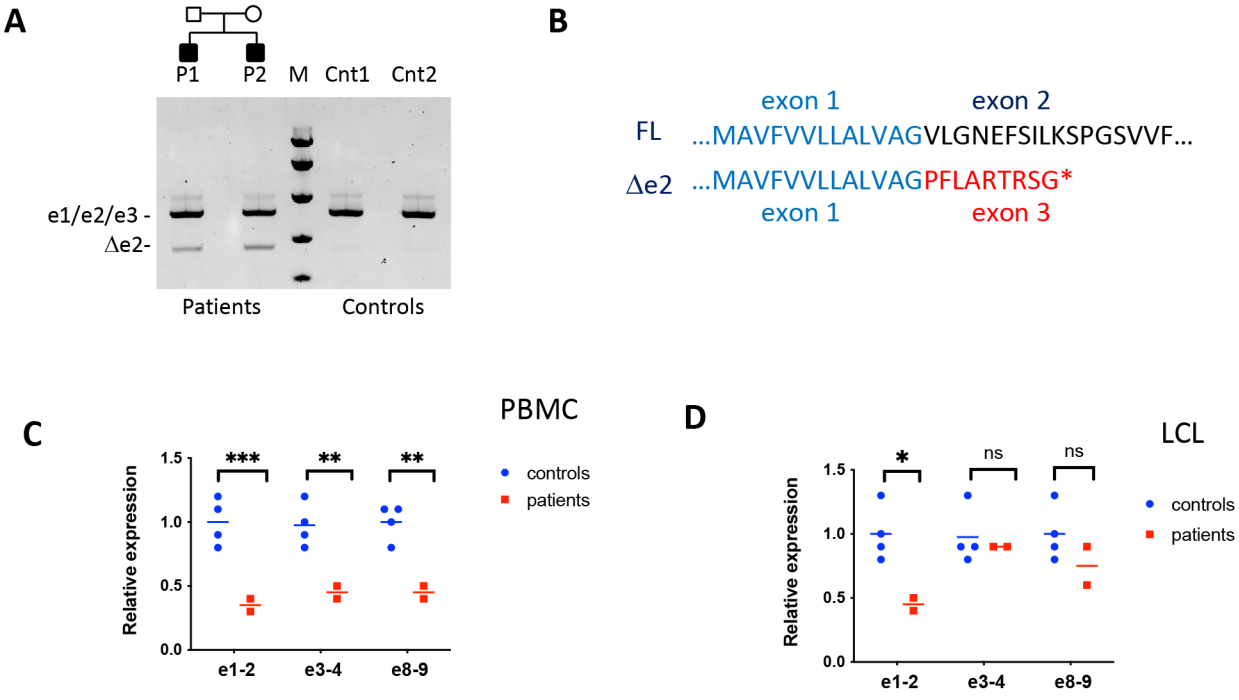

Figure 1.

The c.168+6T>A variant affects exon 2 splicing reducing ATP6AP2 full-length transcript. (A) Gel-resolved products of ATP6AP2 transcripts expressed in PBMC. RT–PCR was performed with ATP6AP2 primers positioned in exons 1 and 3. e1/e2/e3 - transcript containing normally spliced exons 1, 2 and 3; Δe2 – transcript lacking exon 2. P1, P2 - patients carrying c.168+6T>A; Cnt1, Cnt2 - normal controls. M - molecular weight marker. (B) Amino acid sequence of full length (FL) and Δe2 splice isoforms with exon 1/2 and exon 1/3 junctions, respectively. (C-D) Quantification of ATP6AP2 transcripts in PBMC and LCL by qRT-PCR with TaqMan assays detecting exon 1/2, 3/4 and 8/9 junctions. Expression levels were normalized to the mean of the control group. ** p-value < 0.01; *** p-value < 0.001, two-way ANOVA, Sidak's multiple comparison test.

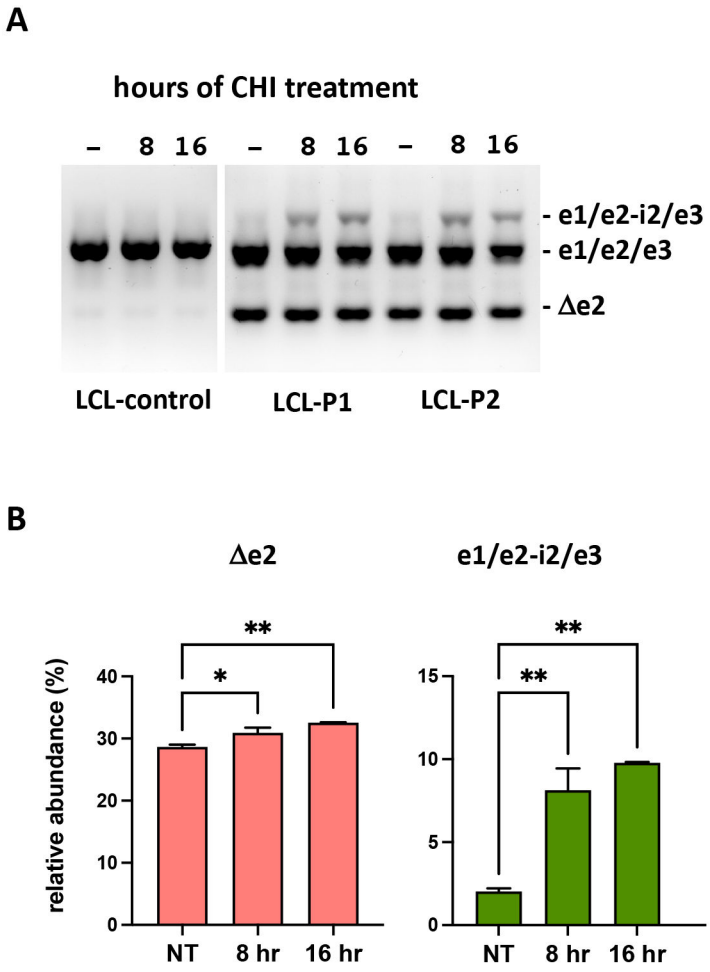

Figure 2.

Regulation of ATP6AP2 splice isoforms by nonsense-mediated RNA decay. (A) Gel-resolved products of ATP6AP2 transcripts expressed in LCL treated with cycloheximide (CHI, 100 ug/ml for 8 and 16 hours). RT–PCR was performed with ATP6AP2 primers positioned in exons 1 and 3. e1/e2/e3 - transcript containing normally spliced exons 1, 2 and 3; Δe2 – transcript lacking exon 2; e1/e2-i2/e3 - transcript in which exon 2 is adjoined with intron 2 sequence. (B) Quantification of the gel shown in A. NT - untreated samples. P1, P2 - patients carrying c.168+6T>A; LCL-control - LCL with reference variant. * p-value < 0.05; ** p-value < 0.01, one-way ANOVA, Dunnett's multiple comparison test.

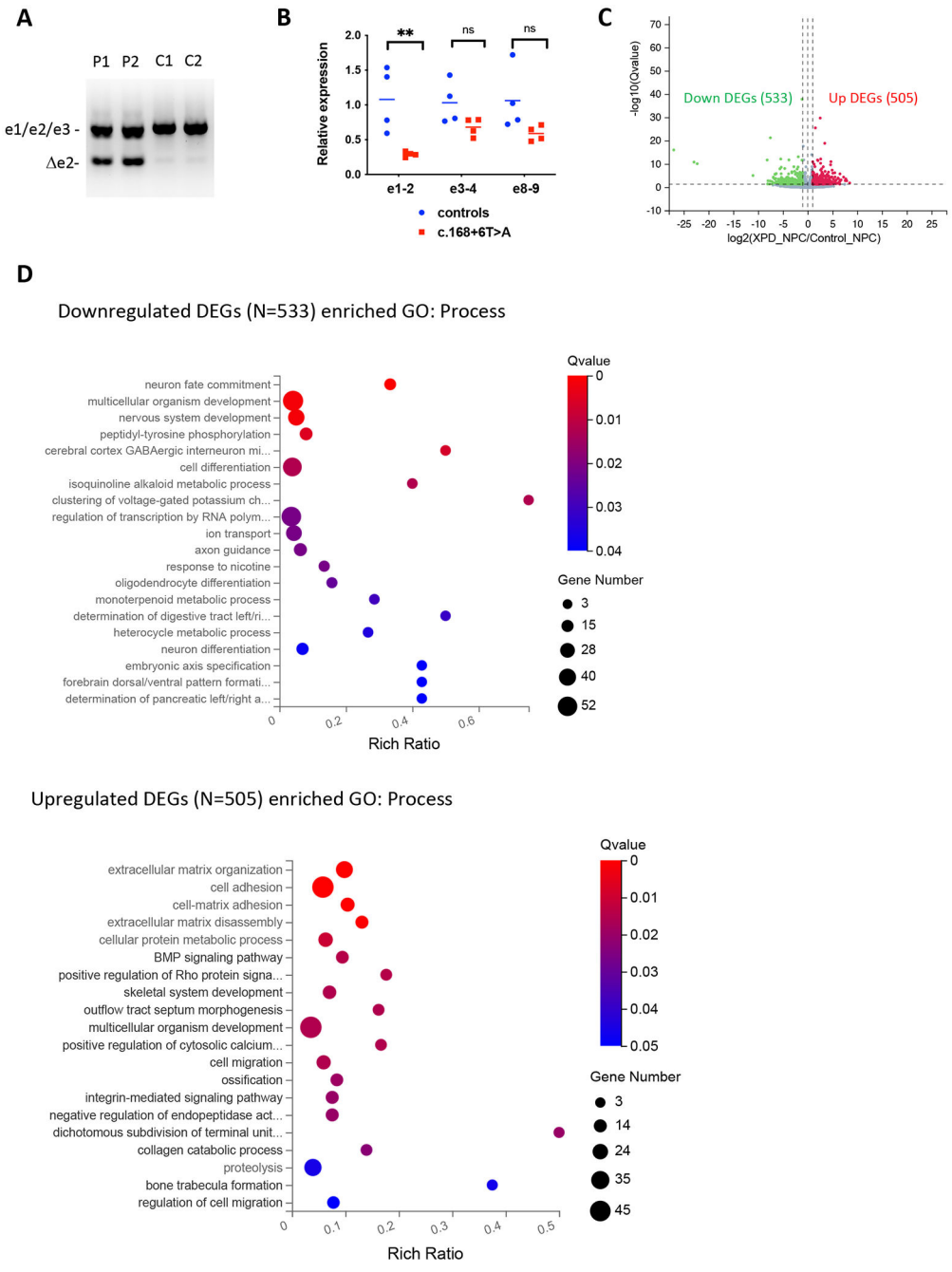

Figure 3.

ATP6AP2 deficit affects multiple pathways in NPCs. (A) Gel-resolved products of ATP6AP2 transcripts expressed in iPSC-derived NPCs. RT–PCR was performed with primers positioned in exons 1 and 3. e1/e2/e3 - transcript containing normally spliced exons 1, 2 and 3; Δe2 – transcript lacking exon 2. C1, C2 – controls; P1, P2 – patients. (B) Quantification of ATP6AP2 transcripts in NPCs by qRT-PCR with TaqMan assays detecting exon 1/2, 3/4 and 8/9 junctions. Expression levels were normalized to the mean of the control group. ** p-value < 0.01; ns – non-significant, two-way ANOVA, Sidak's multiple comparison test. (C) Volcano plot of differentially expressed genes (DEGs) identified by

mRNA-seq. (D) Enriched GO: Biological Process pathways visualized by Dr Tom software (BGI).

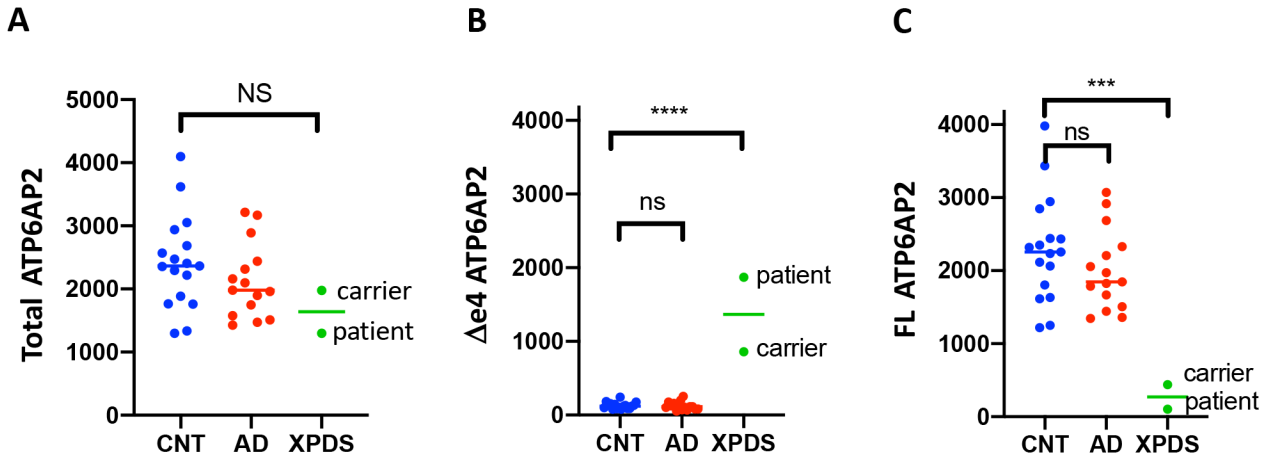

Figure 4.

Aberrant ATP6AP2 splicing in XPDS brains. NanoString analysis of brain RNA of a male XPDS patient and his female sibling carrier of c.345C>T (XPDS, II-2 - patient, II-8 - carrier, see Figure S7), age-matched normal controls (CNT, N=17) and patients with AD (AD, N=15). (A) Quantification of total *ATP6AP2* with a probe to the invariant exon 8/9 junction. (B) Quantification of Δe4 with a probe to *ATP6AP2* exon 3/5 junction. (C) FL *ATP6AP2* was calculated by subtracting level of the Δe4 from that of total *ATP6AP2* transcript. *** p-value < 0.001; **** p-value < 0.0001, one-way ANOVA, Dunnett's multiple comparison test.

Table 1.

Disease-associated genes identified by DisGeNET among DEGs of blood transcriptome.

GO	Description	Log p-value	Log q-value	Enrichment	Z-score	genes in GO	DEGs in GO	GENES ID
C0002792	Anaphylaxis	−6.8	−2.3	25	12	180	6	CPA3|FCER1A| MS4A2|GATA2| HDC|HP
C0013182	Drug Allergy	−4.8	−0.86	60	13	37	3	FCER1A|MS4A2|GSTM1
C0042109	Urticaria	−4.1	−0.38	18	8	168	4	FCER1A|GSTM1|HDC|HP
C0035242	Respiratory Tract Diseases	−3.8	−0.18	15	7.3	198	4	MS4A2|GSTM1|HP|PBRM1
C0035204	Respiration Disorders	−3.8	−0.17	14	7.1	208	4	MS4A2|GSTM1|HP|PBRM1
C3662483	Allergic sensitization	−3.7	−0.17	26	8.5	85	3	FCER1A|MS4A2|FADS2
C0034935	Babinski Reflex	−3.7	−0.17	14	6.9	218	4	ATXN7|ADGRG1|ATP6AP2|NUBPL
C0037268	Skin Abnormalities	−3.4	0	21	7.6	106	3	HDC|FADS2| AKAP12
C0011615	Dermatitis, Atopic	−3.3	0	5.9	5	751	6	FCER1A|MS4A2|GSTM1|VNN2| FADS2|NPL
C0234162	Cerebellar Dysmetria	−3.2	0	18	6.9	127	3	ATXN7|ADGRG1|ATP6AP2
C0302142	Deformity	−2.9	0	8.5	5.2	350	4	GATA2|ATXN7| ADGRG1|AKAP12
C0242422	Parkinsonian Disorders	−2.8	0	7.9	5	373	4	ATXN7|ATP6AP2|SYNM|CCDC62
C0242383	Age related macular degeneration	−2.7	0	5.4	4.3	685	5	GSTM1|HP| ATXN7|FADS2| ATP6AP2
C0235946	Cerebral atrophy	−2.5	0	6.5	4.4	454	4	ATXN7|ATP6AP2|SYNM| TRAPPC2L
C0002874	Aplastic Anemia	−2.4	0	9.4	4.8	237	3	GATA2|GSTM1| HP
C0030312	Pancytopenia	−2.3	0	8.8	4.6	253	3	GATA2|GSTM1| HP
C0033975	Psychotic Disorders	−2.2	0	5.3	3.8	560	4	GSTM1|ATXN7| PBRM1|NPL
C0740279	Cerebellar atrophy	−2	0	6.9	3.9	321	3	ATXN7|ATP6AP2|NUBPL